Molecular Crystals and Liquid Crystals

Publication details, including instructions for authors and subscription information:
http://www.tandfonline.com/loi/gmcl20

Dielectric permittivity measurements of liquid crystal in the microwave and millimeter wave ranges

Yozo Utsumi [a] & Toshihisa Kamei [a]

[a] Department of Communications Engineering, National Defense Academy, Kanagawa, Yokosuka-shi, Japan

Version of record first published: 18 Oct 2010

To cite this article: Yozo Utsumi & Toshihisa Kamei (2004): Dielectric permittivity measurements of liquid crystal in the microwave and millimeter wave ranges, Molecular Crystals and Liquid Crystals, 409:1, 355-370

To link to this article: http://dx.doi.org/10.1080/15421400490433695

Mol. Cryst. Liq. Cryst., Vol. 409, pp. 355–370, 2004

ISSN: 1542-1406 print/1563-5287 online
DOI: 10.1080/15421400490433695

Taylor & Francis
Taylor & Francis Group

DIELECTRIC PERMITTIVITY MEASUREMENTS OF LIQUID CRYSTAL IN THE MICROWAVE AND MILLIMETER WAVE RANGES

Yozo Utsumi and Toshihisa Kamei
Department of Communications Engineering, National Defense Academy, Hashirimizu 1-10-20, Yokosuka-shi, Kanagawa 239-8686, Japan

The fundamental dielectric properties of nematic liquid crystals were measured in the 3–33 GHz frequency range for the purpose of applying liquid crystals to adaptive devices in the microwave and millimeter-wave ranges. We proposed two kinds of measurement methods. Firstly, we used the cut back method to determine the NLCs' permittivity and loss tangent, which is the first time it has been used for this purpose. Secondly, the dielectric permittivity of nematic liquid crystals used for the microstrip-line devices were determined in the 3–33 GHz frequency range by using a newly developed inductive coupled ring resonator. In addition, the effective alignment coefficient $\eta_a (\eta_a < 1)$ *is proposed for the determination of the effective* $\varepsilon'_{\parallel}$ *(the long axis of the liquid crystal molecules is parallel to the direction of the r.f. electric field* E_{rf}*) because the value of* $\varepsilon'_{\parallel}$ *must be modified to* $\eta_a \varepsilon'_{\parallel}$ *in the microstrip-line structure. This concept is useful for the design of the microstrip-line-type variable delay lines.*

Keywords: cut back method; dielectric properties; effective alignment coefficient; inductive coupled ring resonator; microwave; nematic liquid crystal

INTRODUCTION

The near future will see the fusion of broadcasting and communications, and multimedia and multichannel services will be offered via a variety of transmission schemes. Adaptive technologies that can provide seamless

A part of this research work was supported by the 2002 Hoso Bunka (Broadcasting Culture) Foundation and the 2002 Telecommunications Advancement Foundation. The authors wish to thank Dr. Kohji Toda and Dr. Hiroshi Moritake of Department of Electrical and Electronic Engineering, National Defense Academy for their helpful discussions. The authors also wish to thank Mr. Hirosuke Suzuki of Keycom for his helpful discussions.

Address correspondence to Yozo Utsumi, Department of Communications Engineering, National Defense Academy, Hashirimizu 1-10-20, Yokosuka-shi, Kanagawa 239-8686, Japan.

transmission against changes of the radio environment or transmission modes will therefore become important. Software radio technologies may be suitable for this purpose, but only baseband or intermediate frequencies are available at present.

As adaptive technologies in the high-frequency range, electrically tunable technologies for amplitude, phase or frequency are being developed. In the microwave and millimeter-wave ranges, changing the strength or direction of the external magnetic or electric field applied to magnetics or dielectrics used as transmission media allow us to control the transmission performance (i.e., the amplitude or phase).

Liquid crystals (LC) are attractive for future adaptive microwave and millimeter-wave technologies. In applications like variable delay lines or electric phase shifters [1–4]. The performance of these devices depends on the dielectric properties, i.e., the dielectric permittivity, the birefringence, and the loss tangent, of the LC.

The temperature dependence of the nematic(N)LC dielectric relaxation frequency has been obtained by measuring the frequency performance of permittivity at 100 kHz–several GHz [5], and dielectric relaxation at 300kHz–10GHz [6] has been confirmed. Although refs. [5] and [6] provide useful results in a wide frequency band, on the measurements were done at discrete frequencies, and don't provide the continuous variation of LCs' permittivity frequency performance.

This paper presents a very wide band measurement for dielectric properties, which was done by the cut back method [7] in microwave and millimeter-wave ranges. The permittivity measurement including loss tangent of NLCs corresponds to the continuous frequency variation (3–40 GHz). It also discusses the effects of the dielectric birefringence $\Delta\varepsilon' = \varepsilon'_{\parallel} - \varepsilon_{\perp}$, where $\varepsilon'_{\parallel}$ is the real part of the dielectric permittivity when the long axis of LC molecules is parallel to the direction of the r.f. electric field E_{rf}, and $\varepsilon'_{\perp}$ is the one when the long axis of LC molecules is perpendicular to E_{rf}.

The measurement methods reported in [5–7] used a coaxial guide filled with LC. However, variable delay lines often have a microstrip-line-type structure [2–4]. It is therefore important to determine not only the dielectric permittivity of LCs but also the effective dielectric permittivity $\varepsilon'_{\parallel}$ actually working in microstrip-line-type devices, which is a little bit smaller than the true value of the materials.

The permittivity of the microstrip-line's substrate has been measured by using a capacitive coupled ring resonator [8]. However, in the measurement of the dielectric properties of LCs, DC voltage should be fed to the ring resonator [9]. Therefore, we developed a new inductive coupled ring resonator to which DC voltage is fed via an external bias-T. In this paper, an another new measurement method using an inductive coupled ring resonator was also proposed.

And comparing the results of these two different proposed methods, the effective alignment coefficient η_a was also proposed for the microstrip-line type LC devices.

MEASUREMENT METHOD

1. Cut Back Method Using Coaxial Guides

The cut back method [10,11] has been used for the analysis of optical fiber's transmission performance. Here, we applied it for the measurements of LC dielectric properties. In the cut back method,

$$\left.\begin{aligned} \dot{\varepsilon} &= \varepsilon' - j\varepsilon'' \\ \varepsilon'' &= \varepsilon' \cdot \tan\delta \end{aligned}\right\} \tag{1}$$

where $\dot{\varepsilon}$ is the complex relative permittivity of LC, ε' and ε'' are the real part and imaginary part of $\dot{\varepsilon}$, and $\tan\delta$ is the loss angle. Additionally,

$$\left.\begin{aligned} \gamma &= \alpha \pm j\beta \\ \beta &= \omega \cdot \sqrt{\varepsilon_0\mu_0} \cdot \sqrt{\varepsilon'} \cdot \sqrt{\frac{\sqrt{1+\tan^2\delta}+1}{2}} \end{aligned}\right\} \tag{2}$$

where γ, α, and β are the propagation constant, attenuation constant, and phase constant of the TEM wave that propagates in the coaxial guide filled with LC, ε_0, μ_0 are the permittivity and permeability in a vacuum, and ω is the measured angular frequency. Substituting the following relations, we obtain

$c(light\ velocity) = 1/\sqrt{\varepsilon_0\mu_0}$ and $v_p(phase\ verocity) = \omega/\beta$ into Equation (2),

$$\frac{c}{v_p} = \sqrt{\varepsilon'} \cdot \sqrt{\frac{\sqrt{1+\tan^2\delta}+1}{2}} \tag{3}$$

Since $v_g(group\ velocity) = v_p$ for the TEM wave, we use the group delay $\Delta\tau_g$ [sec.] corresponding to the transmission length ΔL [mm] in the coaxial guide, and $\Delta\tau_c$ [sec.] corresponding to ΔL in the light wave transmission and obtain

$$\frac{c}{v_p} = \frac{c}{v_g} = \frac{\Delta L/v_g}{\Delta L/c} = \frac{\Delta\tau_g}{\Delta\tau_c} \tag{4}$$

where $c = 3 \times 10^{11}$ [mm/ sec]. Then, using Eqs. (3) and (4), we obtain

$$\varepsilon' = \left(\frac{\Delta\tau_g}{\Delta\tau_c}\right)^2 \cdot \frac{2}{\sqrt{1+\tan^2\delta}+1} \tag{5}$$

The attenuation constant α[dB/km] has been obtained as the sum of the conduction loss and the dielectric loss [12]. Then, from Eqs. (52) and (54) in [12],

$$\alpha = 87\frac{\sqrt{f}}{Z_0}\left(\frac{\sqrt{\rho}}{d}+\frac{\sqrt{\rho}}{D}\right) + 91\sqrt{\varepsilon'}\cdot f\cdot\tan\delta \tag{6}$$

where d and D [mm] are the diameters of the inner and outer conductor of the coaxial guide, $\rho[\Omega\cdot\mathrm{mm}^2/\mathrm{km}]$ is the resistivity of the inner and outer conductor, f [MHz] is measurement frequency, and $Z_0[\Omega] = 59.96/\sqrt{\varepsilon'}\cdot\ln(D/d)$.

The transmission loss $L_{(\Delta L)}$ corresponding to the transmission length $\Delta L[mm]$ in the coaxial guide is given by

$$L_{(\Delta L)} = \alpha\cdot\Delta L = \sqrt{\varepsilon'}\cdot\Delta L\cdot\left(1.451\sqrt{f}\cdot\sqrt{\rho}\cdot\frac{D+d}{dD\ln(D/d)}+91f\cdot\tan\delta\right)\times 10^{-6}[dB] \tag{7}$$

The value of $\tan\delta$ is obtained from Eq. (7) as

$$\tan\delta = \frac{1}{91f}\left(\frac{10^6\cdot L_{(\Delta L)}}{\sqrt{\varepsilon'}\cdot\Delta L}-1.451\sqrt{f}\cdot\sqrt{\rho}\cdot\frac{D+d}{dD\ln(D/d)}\right) \tag{8}$$

Substituting ε' of Eq. (5) into Eq. (8), we obtain Eq. (9) as follows.

$$\mathrm{Q} = (\text{the left hand side of Eq. (8)}) - (\text{the right hand side of Eq. (8)}) \tag{9}$$

Setting the initial value of $\tan\delta$ to 0 and then increasing it in small steps (0.001) to a value of 100, we continued the calculation until the value of Q crosses 0 (changes sign) in Eq. (9). The values of $L_{(\Delta L)}$ and $\Delta\tau_g$ corresponding to ΔL are given as the measured values of parameter S_{21} with the vector network analyzer. In determining the value of $\tan\delta$ in this way, ε' can also be obtained by Equation (5). In this calculation, we take into account a computational error of less than $\pm 5\%$ for the value of ε' and $\pm 7\%$ for the value of $\tan\delta$.

The experimental setup for these measurements is shown in Figure 1. As the values of $\Delta\tau_g$ and $L_{(\Delta L)}$, we used those measured for two coaxial guides ($L_1 = 180\,\mathrm{mm}$ and $L_2 = 80\,\mathrm{mm}$) where the LC material fills the gap between the inner conductor ($1\,\mathrm{mm}\phi$) and the outer conductor ($3\,\mathrm{mm}\phi$).

$$L_1 - L_2 = \Delta L\,[\mathrm{mm}] \tag{10}$$

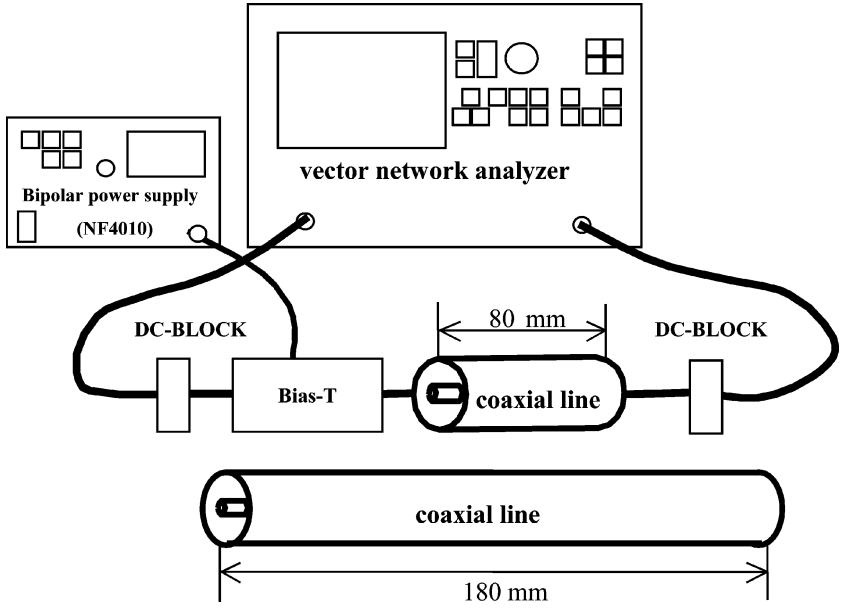

FIGURE 1 Experimental setup of cutback method for measurements of the dielectric properties of LC.

In the first step, the dielectric properties are measured without DC electric field E_0 between the inner and outer conductors of the coaxial guides. In this case, the LC molecules randomly align with the rf electric field E_{rf} of the TEM wave, where ε'_a is the real part of the relative permittivity and $\tan\delta_a$ the loss angle. Next, the dielectric properties are measured with E_0 applied to the gap (1 mm) between the inner and outer conductors. When the applied voltage exceeds the threshold value, the long axis of the LC molecules aligns parallel to the direction of E_{rf}. The value of the real part of the relative permittivity and the loss angle of LC saturate as $\varepsilon'_{\parallel}$ and $\tan\delta_{\parallel}$, respectively. In this measurement, changing the value of the applied voltage between 0–150 V, the measured value with 150 V applied where saturated enough, is defined as $\varepsilon'_{\parallel}$ and $\tan\delta_{\parallel}$. Finally, the real part of the permittivity $\varepsilon'_{\perp}$ and the loss angle $\tan\delta_{\perp}$, where the long axis of the LC molecules is perpendicular to the direction of E_{rf}, are obtained. Although $\varepsilon'_{\perp}$ and $\tan\delta_{\perp}$ can not be measured directly, their values can be determined by calculation using the measured ε'_a, $\varepsilon'_{\parallel}$, $\tan\delta_a$ and $\tan\delta_{\parallel}$ as follows [13]:

$$\varepsilon'_{\perp} = \frac{3\varepsilon'_a - \varepsilon'_{/\!/}}{2} \tag{11}$$

$$\tan\delta_{\perp} = \frac{3\varepsilon'_a \tan\delta_a - \varepsilon'_{/\!/} \tan\delta_{/\!/}}{2\varepsilon'_{\perp}} \tag{12}$$

2. Resonance Method Using Inductive Coupled Ring Resonator

Figure 2 shows the structure of the inductive coupled ring resonator with LC material as microstrip-line substrate. The ring resonator is connected with 50-Ω input and output terminals by inductive coils whose diameter is 80 μm. This microwave circuit is patterned on ordinary 0.25 mm-thick microwave dielectric substrate (PILLAR PC-CRAD) whose relative permittivity is 3.0. The patterned side of the dielectric substrate and the upper side of the ground conductor are processed with rubbed polyimide spin coating. The outer and inner diameters of the ring resonator are denoted as D_1 and D_2 respectively, the length of coupling inductance coil as l, the thickness of the LC layer as t.

When the DC electric field E_0 is applied between the ring resonator and ground plane, the long axis of the LC's molecules becomes parallel to the direction of the r.f. electric field E_{rf} in the quasi TEM mode, the relative dielectric permittivity is denoted as $\varepsilon'_{\parallel}$. And when the long axis becomes

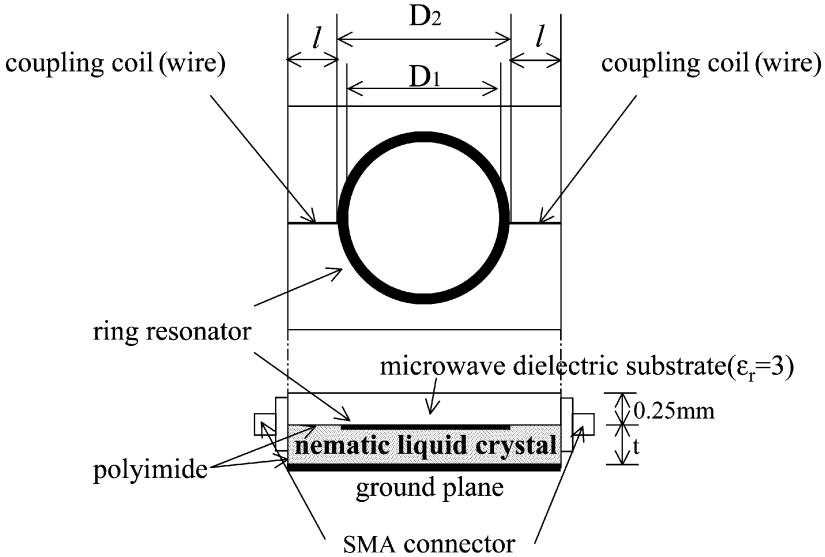

FIGURE 2 The Inductive coupled ring resonator with LC material as the microstrip-line substrate.

perpendicular to the direction of E_{rf} due to the alignment force of polyimide layers without E_0, it is denoted as $\varepsilon'_{\perp}$.

The LC filling the gap between the ring resonator pattern and the ground plane can be considered a microstrip-line substrate.

Figure 3 shows the microwave measurement setup. Scattering parameter S_{21} (transmission coefficient) was measured in the frequency range of 3–33 GHz with a vector network analyzer. The DC bias voltage was applied to the ring resonator via the external bias-T.

By fitting the simulated results to the measured frequency performance of S_{21} at every peak of the inductive coupled ring resonator, we can decide the frequency performances of the measured NLCs' $\varepsilon'_{\parallel}$ and $\varepsilon'_{\perp}$.

The simulator used in these measurements is the electromagnetic simulation function of Microwave Office 2002 (Applied Wave Research, Inc.). The electromagnetic analysis performed by this software uses the method of moments (MoM). In Figure 2, the ring section of the ring resonator is partitioned by a small grid in which surface current is assumed to flow, and the current distribution is determined using MoM [14].

The analysis model employs a ring similar in size to that used in the experiment. The small grid here consists of 120×200 cells for a ring width of 0.5 mm and 60×100 cells for a ring width of 2 mm. Given that grid size is smaller than ring width by half or more for the sake of improving computational accuracy, the number of grid cells here is determined so that grid size becomes 0.25 mm and 0.5 mm, respectively. In addition, frequency runs

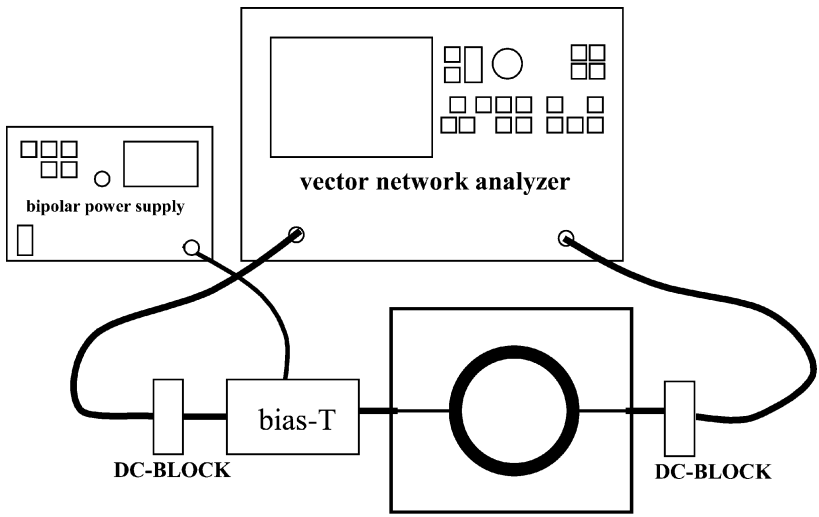

FIGURE 3 Experimental setup for measurements of the dielectric permittivities of LC.

from 3 to 33 GHz in 0.05 GHz steps. Though dependent on computer performance, analysis time for the model shown in Figure 2 is about 10 hours.

RESULTS AND CONSIDERATIONS ON DIELECTRIC PROPERTIES' MEASUREMENTS

1. Dielectric Permittivities in 3–40 GHz with the Cut Back Method

Dielectric properties of five kinds of NLC; BL006, BL048, BL011, BL005 and MLC11000-100 (made by MERCK) measured in the 3–40 GHz range, corresponding to the continuous frequency variation, are summarized in Table 1. The values of $\varepsilon'_{\parallel}$ and $\varepsilon'_{\perp}$ are approximately constant in a very wide frequency range as shown in Figure 4.

The dielectric birefringence $\Delta\varepsilon'$ is defined as

$$\Delta\varepsilon' = \varepsilon'_{\parallel} - \varepsilon'_{\perp} \tag{13}$$

The obtained values of $\Delta\varepsilon'$ are 0.4–0.8 for the five kinds of materials as show in Figure 4. And $\tan\delta_{\parallel} < 0.05$, $\tan\delta_{\perp} < 0.14$ in this frequency range as shown in Figure 5. The value of $\tan\delta_{\perp}$ is larger than that of $\tan\delta_{\parallel}$, because the dielectric relaxation frequency of $\varepsilon'_{\perp}$ is larger than $\varepsilon'_{\parallel}$'s, and the increment of dielectric loss caused by relaxation in the low-frequency range gives the effect to the microwave range. We confirmed the dielectric relaxation for three kinds of NLCs by another experiment in the low frequency range. The dielectric relaxation of $\varepsilon'_{\parallel}(\varepsilon''_{\parallel})$ near 1 MHz (BL011), 2 MHz (BL005), 2.5 MHz (MLC11000–100) and that of $\varepsilon'_{\perp}(\varepsilon''_{\perp})$ near 100 MHz(BL011), 80 MHz (BL005), 70 MHz (MLC11000–100) was confirmed, respectively.

From Figures 4 and 5, it is evident that there is no dielectric relaxation and the value of $\Delta\varepsilon'$ seems to stay approximately constant in the frequency range of 3–40 GHz. This suggests that the transmission

TABLE 1 Dielectric Properties of NLC(MERCK) Used for our Measurements

	BL006	BL011	BL048	BL005	MLC11000–100
N-I(°c)	+113	+62	+100	+64	+75
$\Delta\varepsilon'$ (1 kHz, 20°c)	+17.3	+16.2	+16.8	+15.4	+7.4
$\varepsilon_{\parallel}$ (1 kHz, 20°c)	22.8	22.4	22.0	21.4	11.6
Viscosity (mm^2/sec., 20°c)	71	63	47	32	17

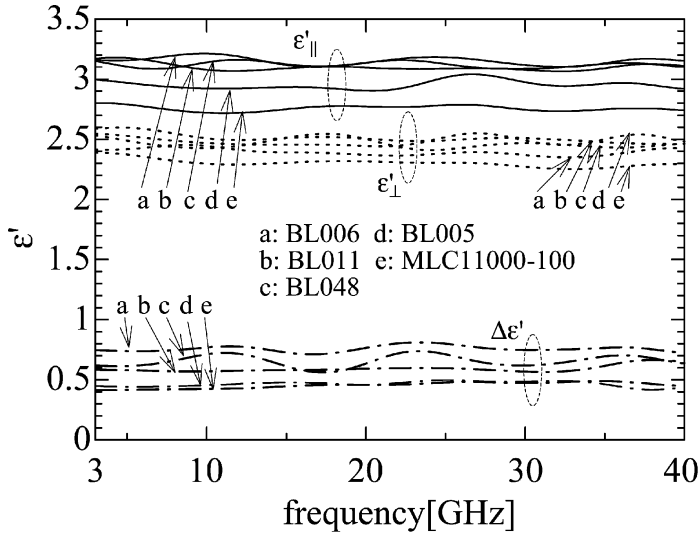

FIGURE 4 Frequency performances of LC's permittivity$\varepsilon'_{\parallel}$, $\varepsilon'_{\perp}$, $\Delta\varepsilon'$).

performance of adaptive devices using these LCs can be controlled by the applied voltage in a wide frequency range. Among the measured materials, BL006 had the largest $\Delta\varepsilon'$, 0.8, and MLC11000-100 the smallest, 0.4.

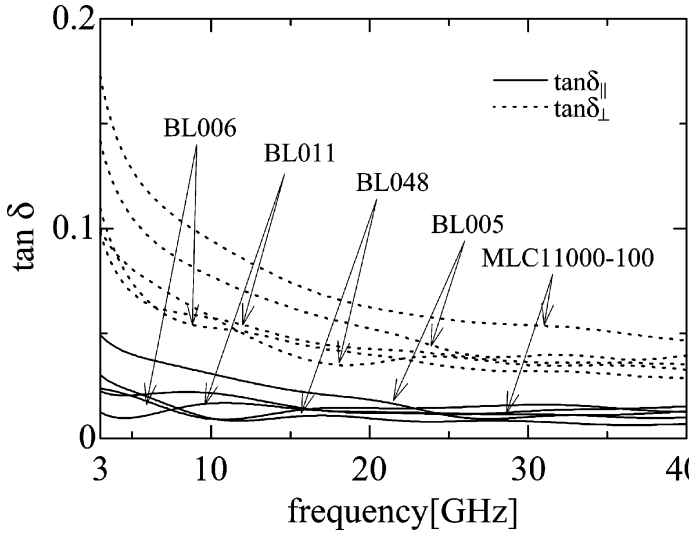

FIGURE 5 Frequency performances of LC's loss tangent ($\tan\delta_{\parallel}$, $\tan\delta_{\perp}$).

A variable delay line using BL006 has small insertion loss, because the delay line can be made short enough to keep the same phase shift. Comparing Table 1 with Figure 4, one can see that materials whose $\Delta\varepsilon'$ (measured at 1 kHz) is big, give a big value of $\Delta\varepsilon'$ also in the microwave range.

2. Dielectric Permittivities in 3–33 GHz with the Resonance Method

The dielectric permittivities of three NLCs, BL006, BL048, MLC11000-100 (MERCK), were determined by fitting the simulation results to the experimental frequency performances of $\varepsilon'_{\parallel}$ and $\varepsilon'_{\perp}$.

The frequency performance of $\varepsilon'_{\parallel}$ and $\varepsilon'_{\perp}$ was measured at the bias voltage 50 V and 0 V, respectively. In the measurements, $\varepsilon_r = 3.0$, $D_1 = 16\,\text{mm}$, $D_2 = 12\,\text{mm}$, $w = (D_1 - D_2)/2 = 2\,\text{mm}$, $l = 6.5\,\text{mm}$, the diameter of coil $= 80\,\mu\text{m}$, and $t = 320\,\mu\text{m}$ (See Fig. 2). The dielectric properties of the three NLCs(MERCK) used for measurements are summarized in Table 1.

The measured S_{21} frequency performance of the ring resonator filled with BL006 when bias voltage was applied and there was no rubbing polyimide layer is shown in Figure 6 along with the simulated value (NLC permittivity = 3.17: average value of $\varepsilon'_{\parallel}$ by cut back method). In this

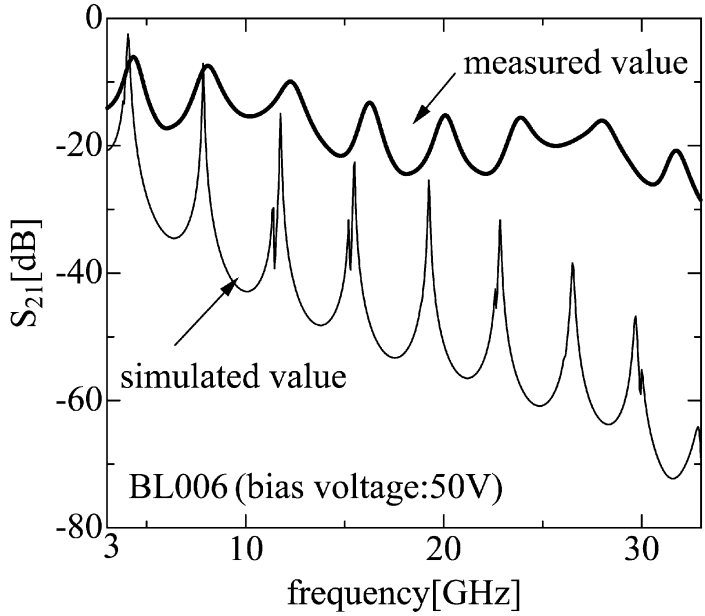

FIGURE 6 Measured and simulated (NLC permittivity = 3.17) S_{21} performance of the ring resonator filled with BL006 NLC with bias voltage.

case, the NLC under the ring resonator plays the role of the microstrip-line substrate with $\varepsilon'_{\parallel}$ permittivity. In order to realize the permittivity $\varepsilon'_{\parallel}$ where the long axis of the LC's molecules becomes parallel to the direction of E_{rf}, we removed the rubbing polyimide layer because the alignment force against the NLC molecules caused by E_0 is not so strong in the area except just under the ring resonator, as shown in Figure 8. The measured value of each resonant frequency is a little bit bigger than the simulated one.

The S_{21} of the ring resonator filled with BL006 NLC when bias voltage was not applied and there was a rubbing polyimide layer, is shown in Figure 7 along with the simulated value (NLC permittivity = 2.38: average value of $\varepsilon'_{\perp}$ by cut back method). In this case, the NLC plays the role of the microstrip-line substrate with $\varepsilon'_{\perp}$ permittivity. The measured value of each resonant frequency closely coincides with the simulated one.

By fitting the simulated result to the experimental one at every peak as shown in Figures 6 and 7, we obtained the frequency performance of BL006's permittivity ($\varepsilon'_{\parallel}$, $\varepsilon'_{\perp}$, $\Delta\varepsilon'$) shown in Figure 9, where the data is shown along with the results for the cut back method. The frequency performance of BL048's and MLC11000-100's permittivity is also shown in Figures 10 and 11.

In Figures 9, 10 and 11, measured values of $\varepsilon'_{\perp}$ closely coincide with the results for the cut back method. The measured values are a little bit smaller

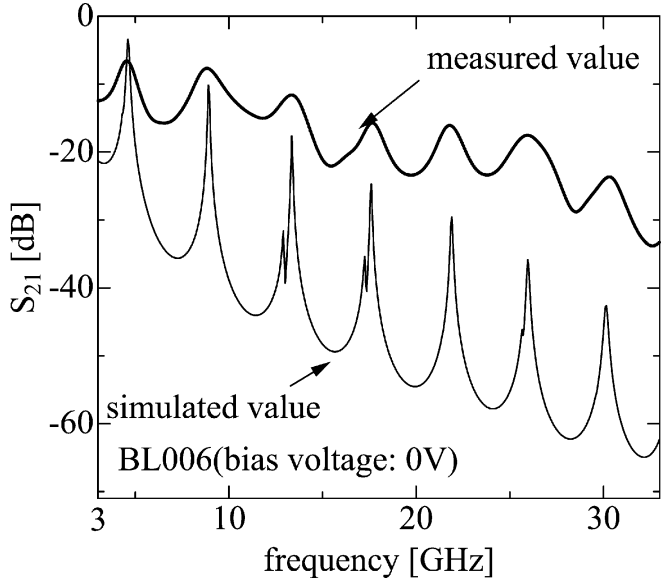

FIGURE 7 Measured and simulated (NLC permittivity = 2.38) S_{21} performance of the ring resonator filled with BL006 NLC without bias voltage.

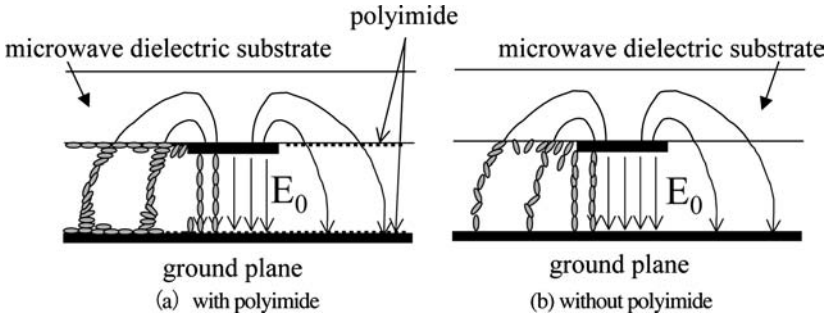

FIGURE 8 Image of alingment force against NLC molecules caused by E_0.

because the perfect alignment of NLC's molecules is not achieved except just under the ring resonator even without a polyimide layer as shown in Figure 8(b).

Also the effective values of $\Delta\varepsilon'$ decreased to about 0.5 for BL006, 0.4 for BL048, and 0.3 for MLC11000-100.

CONSIDERATIONS ON THE EFFECTIVE ALIGNMENT COEFFICIENT

Filling coaxial guides with NLCs, the material's values of $\varepsilon'_{\parallel}$ and $\varepsilon'_{\perp}$ were obtained by the cut back method.

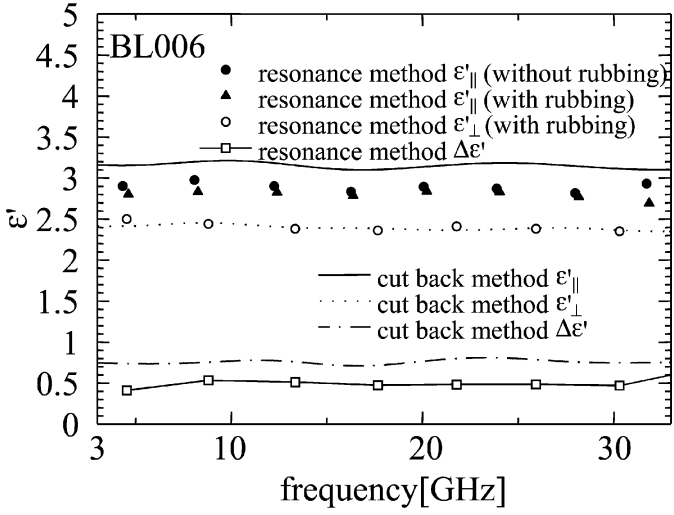

FIGURE 9 Measured values of BL006's permittivity.

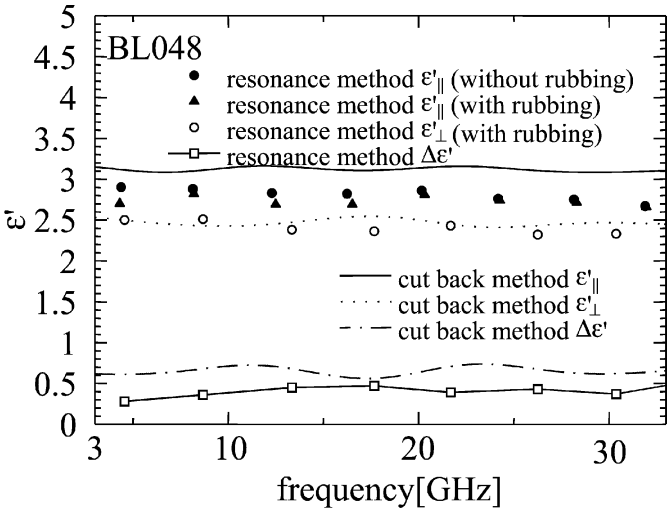

FIGURE 10 Measured values of BL048's permittivity.

However, most applications, like variable delay lines, have microstrip-line structures in microwave and millimeter-wave ranges. In these microstrip-line-type applications, the direction of NLC's molecules can not be perfectly controlled by a bias voltage as shown in Figure 8. As a result, the value of $\varepsilon'_{\parallel}$ becomes a little bit smaller than the true value. Actual

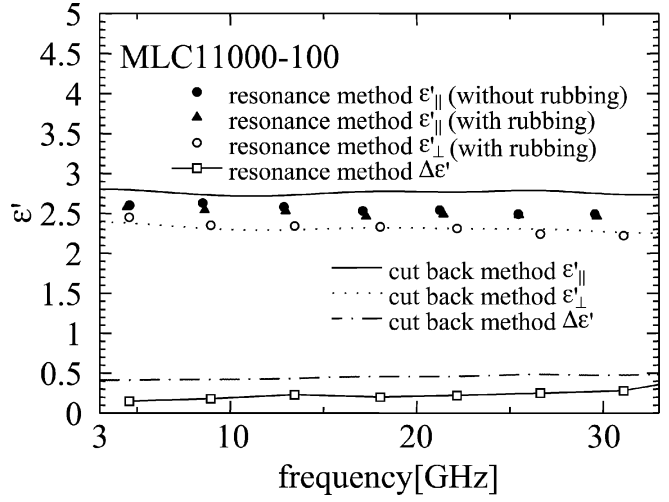

FIGURE 11 Measured values of MLC11000-100's permittivity.

devices should be designed by using the effective value in the microstrip-line structure. Therefore, the true value of $\varepsilon'_{\parallel}$ should be quantitatively modified by the effective alignment coefficient (η_a), which mainly depends on the microstrip-line structure and NLC's viscosity. Here, the true value of $\varepsilon'_{\parallel}$ is assumed to be the one measured by the cut back method. Using the true value of $\varepsilon'_{\parallel}$, $\varepsilon'_{\parallel c}$ and the effective value of $\varepsilon'_{\parallel}$ in microstrip-line structure, $\varepsilon'_{\parallel s}$, we obtain

$$\eta_a = \frac{\varepsilon'_{\parallel s}}{\varepsilon'_{\parallel c}} \tag{14}$$

where $\eta_a < 1$.

Figure 12 shows the effective alignment coefficient η_a corresponding to several NLC's viscosities at 8 GHz. The solid line indicates η_a for NLC's $\varepsilon'_{\parallel}$ without polyimide layer, and the dotted line for η_a with a polyimide layer. It is evident the large value of viscosity makes it difficult to change the direction of NLC molecules from the initial condition to the E_0 direction in the area except just under the ring resonator as imaged in Figure 8. Both values of η_a decrease to about 0.89–0.95 as shown in Figure 13.

The value of $\varepsilon'_{\parallel}$ decreases because $\eta_a(\eta_a < 1)$, and, on the other hand, $\varepsilon'_{\perp}$ has the same value obtained by cut back method. Therefore, $\Delta\varepsilon'(= \varepsilon'_{\parallel} - \varepsilon'_{\perp})$ decreases as shown in Figures. 9,10, and 11.

Figure 13 shows the effective alignment coefficient η_a corresponding to three kinds of characteristic impedances in ring resonators. It is evident

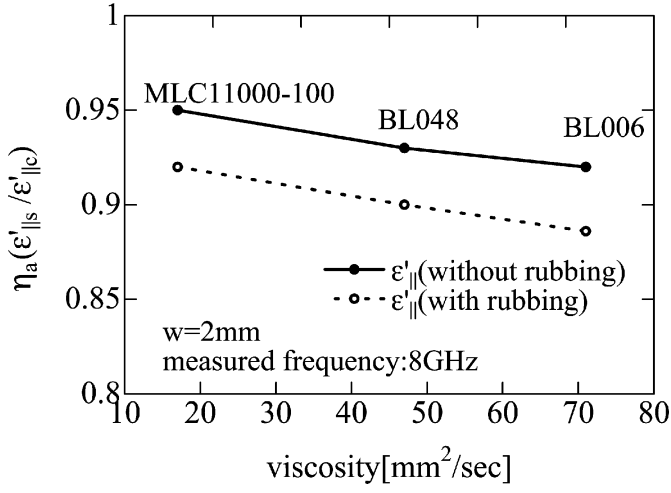

FIGURE 12 Effective alignment coefficient η_a vs. viscosity in microstrip-line type LC devices.

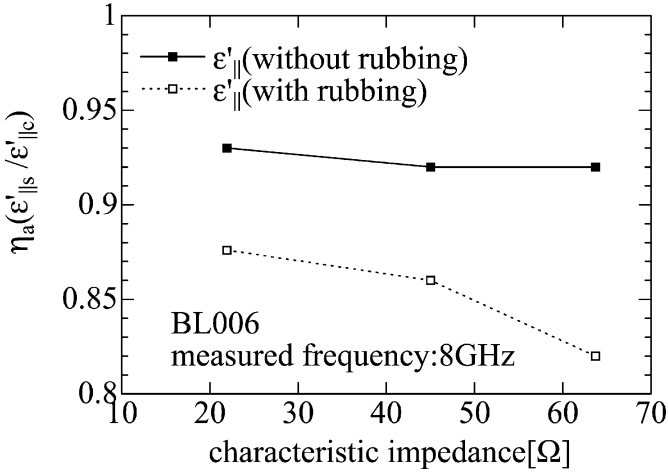

FIGURE 13 Effective alignment coefficient η_a vs. characteristic impedance in microstrip-line type LCdevices.

that η_a for a low-characteristic-impedance microstrip-line having a lot of energy in the area just under the strip conductor is larger than that for a high characteristic-impedance structure. For example, in designing a $50\,\Omega$ microstrip-line-type variable delay line with BL006, the value of $\varepsilon'_{\parallel}$ decreases to 85% of its true value because $\eta_a = 0.85$.

CONCLUSION

Two kinds of measurement methods for determining LC's dielectric properties in the microwave and millimeter-wave ranges were propsed. The cut back method using coaxial guides is suitable for determining the dielectric properties of LC material itself, and the resonance method using an inductive coupled ring resonator is for determining the effective dielectric permittivity of microstrip-line type LC devices. Comparing these results, the concept of an effective alignment coefficient η_a was also proposed. It was shown that the effective NLC permittivity $\varepsilon'_{\parallel}$ in microstrip-line structure applications has a value that is a little bit smaller than the material's true value quantitatively.

REFERENCES

[1] Lim, K. C., Margerum, J. D., & Lackner, A. M. March (1993). *Appl. Phys. Lett.*, *62*(10), 1065–1067.

[2] Dolfi, D., Labeyrie, M., Joffre, P., & Huignard, J. P. May (1993). *Electron. Lett.*, *29*(10), 926–928.

[3] Guerin, F., Chappe, J. M., Joffre, P., & Dolfi, D. July (1997). *Jpn. J. Appl. Phys.*, *36*(7A), part.1, 4409–4413.
[4] Takao Kuki, Hideo Fujikake, Toshihiro Nomoto, & Yozo Utsumi, Feb.(2001). *Trans. IEICE. C*, *J84*-C, (2), 90–96.
[5] Bose, T. K., Campbell, B., & Yagihara, S. Dec.15,(1987). *Physical Rev. A*, *36*(12), 5767–5773.
[6] Nozaki, R., Bose, T. K., & Yagihara, S. Dec.15, (1992). *Physical Rev.A*, *46*(12), 7733–7737.
[7] Kamei, T., Utsumi, Y., Moritake H., & Toda, K. July (2002). "Fundamental properties of liquid crystal in microwave and millimeter wave range." Abstract of ILCC2002, 72.
[8] Semouchkina, E., Cao, W., & Lanagan, M. May.25, (2000). *Electronics Lett.*, *36*(11), 956–958.
[9] Utsumi, Y. & Kamei, T. July (2002). "Dielectric permittivity measurements of liquid crystal in the microwave range using an inductive coupled ring resonator." Abstract of ILCC2002, 73.
[10] American Society for Testing and Materials (ASTM), EIA-455-78A-90, MIL-STD-2196-(SH), Glossary of fiber opticterms.
[11] Lee, J. H., Lee, W. J., & Park, N. Dec. (1998). *IEEE Photonics Tec. Letters*, *10*(12), 1721–1723.
[12] Corti, G. & Tizzi, G. Sept. (1977). *Alta frequenza*, *XLVI*, (9), 213E 389–223E E399.
[13] Japan society for the Promotion of Science 142 nd Committee. Liquid crystal device handbook, Nikkan Kogyo Shinbun; 1989(in Japanese).]
[14] Harrington, R.F. (1968). *Field computation by moment methods*, The Macmillan Co.: N.Y., 1–61.